Nuclear Instruments and Methods in Physics Research A 609 (2009) 227–234

Contents lists available at ScienceDirect

Nuclear Instruments and Methods in Physics Research A

journal homepage: www.elsevier.com/locate/nima

Trigger electronics of the new Fluorescence Detectors of the Telescope Array Experiment

Yuichiro Tameda [a,*], Akimichi Taketa [b], Jeremy D. Smith [c], Manobu Tanaka [d], Masaki Fukushima [b], Charles C.H. Jui [c], Ken'ichi Kadota [f], Fumio Kakimoto [a], Takeshi Matsuda [d], John N. Matthews [c], Shoichi Ogio [e], Hiroyuki Sagawa [b], Nobuyuki Sakurai [b], Tatsunobu Shibata [b], Masahiro Takeda [b], Stanton B. Thomas [c], Hisao Tokuno [b], Yoshiki Tsunesada [a], Shigeharu Udo [b]

[a] Graduate School of Science and Engineering, Tokyo Institute of Technology, Meguro, Tokyo 152-8551, Japan
[b] Institute for Cosmic Ray Research, University of Tokyo, Kashiwa, Chiba 277-8582, Japan
[c] Institute for High Energy Astrophysics and Department of Physics, University of Utah, Salt Lake City, UT 84112-0830, USA
[d] Institute of Particle and Nuclear Studies, KEK, Oho, Tsukuba, Ibaraki 305-0801, Japan
[e] Graduate School of Science, Osaka City University, Sumiyoshi, Osaka 558-8585, Japan
[f] Faculty of Knowledge Engineering, Musashi Institute of Technology, Setagaya, Tokyo 158-8557, Japan

ARTICLE INFO

Article history:
Received 28 November 2008
Received in revised form
5 July 2009
Accepted 5 July 2009
Available online 11 August 2009

Keywords:
Ultra High Energy Cosmic Rays
Extensive air shower
Fluorescence light
Event trigger
Monte Carlo technique

ABSTRACT

The Telescope Array Project is an experiment designed to observe Ultra High Energy Cosmic Rays via a "hybrid" detection technique utilizing both fluorescence light detectors (FDs) and scintillator surface particle detectors (SDs). We have installed three FD stations and 507 SDs in the Utah desert, and initiated observations from March 2008. The northern FD station reuses 14 telescopes from the High Resolution Fly's Eye, HiRes-I station. Each of the two southern FD stations contains 12 new telescopes utilizing new FADC electronics. Each telescope is instrumented with a camera composed of 256 PMTs. Since the detectors are composed of many PMTs and each PMT detects fluorescence photons together with the vast amount of night sky background, a sophisticated triggering system is required. In this paper, we describe the trigger electronics of these new FD stations. We also discuss performance of the FDs with this triggering system, in terms of efficiencies and apertures for various detector configurations.

1. Introduction

Soon after the discovery of the cosmic microwave background radiation [1], it was predicted that if Ultra High Energy Cosmic Rays (UHECRs) were of extragalactic origin, there would be an end to the observed cosmic ray spectrum [2,3]. Cosmic rays with primary energies greater than $\sim 10^{19.5}$ eV would be subject to strong energy losses during their propagation resulting from pion production in their interactions with CMB photons. This is called the GZK cutoff.

The AGASA experiment [4,5] reported the detection of 11 "super-GZK" events. However, for the AGASA exposure, the group predicted 2.1 events [6,7] under the assumption a uniform source distribution being acted upon by a GZK-cutoff. On the other hand, the High Resolution Fly's Eye (HiRes) experiment [8], with a larger exposure at the highest energies, reported an energy spectrum with a cutoff consistent with theoretical predictions (5σ) [9,10].

The inconsistencies between the AGASA and the HiRes results also extend to lower energies. It may be possible to attribute some, but not all, of these differences to systematic errors in the energy scales of the experiments. In observing cosmic ray air showers via a surface detector array, such as AGASA, one samples the density of particles from the shower when they reach the Earth's surface. A surface array cannot directly observe the longitudinal development of the air showers; this inevitably leads to systematic uncertainties in the energy determination due to shower development fluctuations and differences in the mass composition of the primary nuclei. On the other hand, when using the atmospheric fluorescence detection technique, such as in HiRes, one can directly measure the shower's longitudinal development and determine the primary energy with calorimetric methods. In this case, however, there are other sources of uncertainties in the energy determination, for example transparency of the atmosphere and its variation with time or fluorescence yield at different heights and atmospheric conditions.

A complementary approach utilizing the two different detection methods delivers a large area detector with improved geometrical and energy resolution. Such "hybrid" detection also

* Corresponding author. Tel.: +81 3 5734 2462; fax: +81 3 5734 2756.
E-mail address: tame@cr.phys.titech.ac.jp (Y. Tameda).

0168-9002/$ - see front matter © 2009 Elsevier B.V. All rights reserved.
doi:10.1016/j.nima.2009.07.093

offers the opportunity to perform a direct comparison to investigate the sources of the differences between the AGASA and the HiRes spectrum. The Telescope Array (TA) Collaboration, which includes members from AGASA and HiRes, has started operation of a large scintillator surface detector (SD) array [11,12] and three Fluorescence Detector (FD) stations [13] in the west desert of Utah (See Fig. 1). The goal is to clarify the origin and astrophysics of UHECRs, with both air shower detection techniques. The Pierre Auger Observatory [14], located in Argentina, also uses surface detectors of 3000 km^2 area and four Fluorescence Detectors.

One advantage of the experiment is that the TA site is located in the northern hemisphere, where the effects of the galactic magnetic field on the trajectories of UHECRs are smaller than in the case for the southern hemisphere [15]. Additionally, the Telescope Array has the same view of the sky as the HiRes experiment and it has a large overlap with the view of AGASA. Therefore, by tracing the arrival directions back to original sources of the UHECRs, we can investigate the anisotropy as reported by AGASA [16,17] and HiRes [18,19], with improved angular accuracy.

The northernmost of the three TA FD observatory sites reuses 14 telescopes from the HiRes-I experiment [20]. This will permit a direct comparison to the HiRes energy scale and analysis. The two southern FD stations are each instrumented with 12 telescopes newly developed for this experiment. The new TA FD telescopes consist of composite spherical mirrors and an imaging camera composed of 256 PhotoMultiplier Tubes (PMTs).

The new FD telescopes also have new FADC electronics which were developed for them. The new trigger electronics for this system are partly based upon the HiRes-I trigger, but expand upon the logic which HiRes-I used taking advantage of the increased capacity which the intervening years have brought to electronics.

The trigger electronics are composed of two classes of modules: Track Finders (TFs) and Central Trigger Distributors (CTDs). Both modules make use of CPLD (Complex Programmable Logic Device) and FPGA (Field Programmable Gate Array) devices. Each camera has its own TF module whose job is to examine fired PMT patterns to find the signal of an air shower track in a camera and, once identified, to send an alert to the CTD. Each FD station requires only one CTD module; it watches alerts from the TFs and sends trigger signals to the camera DAQ to record waveform data from the PMTs.

In this paper, we describe the trigger electronics developed for the new FD telescopes. In Section 2, we briefly describe the characteristics of the telescopes at the southern two FD stations and outline the electronics. Sections 3 and 4 provide detailed descriptions of the TF and CTD modules. In Section 5, the electronics are evaluated via Monte Carlo (MC) aperture calculations. This is done for various detector configurations, i.e., monocular, stereo, and hybrid observation with the SD array. The results are summarized in Section 6.

2. The FD telescopes and their triggering processes

The southern two Fluorescence Detector (FD) stations (Black Rock and Long Ridge) are each instrumented with 12 new telescopes. Each telescope consists of a composite mirror and a camera. The 3.3 m diameter mirror is composed of 18 hexagonal segments which have a focal length of 3.0 m and a spot size of 30 mm on the focal plane. The camera for the telescope, installed on the focal plane, is composed of 256 hexagonal PMTs (HAMAMATSU R9508). The PMTs have a flat to flat side distance of 60 mm, so the sensitive area of the camera is about 1 m^2. Each PMT pixel views approximately 1° of sky and the camera has a field of view of 15° in elevation and 18° in azimuth. The telescopes at each site are installed in a "two ring" geometry; with six telescopes in "ring-1" viewing 108° in azimuth and from 3° to 18° in elevation. The upper ring ("ring-2") has the same azimuthal span, but views elevations from 18° to 33°.

A block diagram outlining the trigger electronics and the data acquisition (DAQ) system for the new FD station is shown in Fig. 2. After passing through a DC-coupled pre-amplifier to enable a direct measurement of the night sky background, the signals from each PMT are sent to Signal Digitizer/Finder (SDF) modules [21]. This is the front-end of the FD electronics which further amplifies and then digitizes the output from the PMTs. Finally, the SDF searches for significant signals above threshold such as those caused by fluorescence photons associated with air showers.

One SDF module processes 16 input channels and 16 modules are installed for each camera—256 PMTs. The SDF has a 12 bit digitizer running at 40 MHz (25 ns/sample). It adds four samples together into a bin, so that it is equivalent to 14 bits at 10 MHz (100 ns/sample). This represents a dynamic range up to 7 K photo-electrons since the typical conversion factor is 2.27 count per photo-electron. To find the signal, the SDF slices the data into 25.6 μs "frames" containing 256 bins of FADC data samples. There is an overlap of 12.8 μs between adjacent frames. In order to extract a signal within a frame, the SDF calculates rolling averages for four time windows (1.6, 3.2, 6.4 and 12.8 μs), and compares them with background levels. If the SDF finds an excess greater than the pre-determined threshold, it sends an alert to the TF module of the camera. This is the "first level" trigger [21]. The average trigger rate is about ~3 Hz with 6 sigma threshold level for the first level trigger.

The TF module collects the first level triggers from all 256 PMTs of the camera via the 16 SDFs. The TF deals with this information as a "hit pattern" of the camera and compares with the trigger pattern table programmed in the RAMs. If a match for a shower track is found, a "second level" trigger signal is sent to the CTD module for the whole station. At this time, when the CTD receives a second level trigger signal from one or more TFs, the module sends a "final" trigger signal to all of the cameras at the station to activate data recording processes for all signal channels. After we have more experience with the electronics, it is likely that we will work to reduce the amount of data which we record.

3. The Track Finder

The TF module processes the hit patterns of one camera in every frame. When it recognizes the hit patterns as an air shower track, it sends the second level trigger to the CTD.

The major components of the TF are one CPLD (XC95288XL), one FPGA (XC2S400E), one configuration ROM (XC18V04) and nine SRAMs (CY7C1041). These devices are assembled onto a 9 U VME printed circuit board. The block diagram of the TF module is shown in Fig. 3.

At each camera, one TF module communicates with the 16 SDFs via the VME bus lines. To form the second level trigger, the TF searches through the PMT hits, determined by the SDFs, looking for patterns in space and time. It recognizes shower tracks on the camera or rejects accidental coincidences caused by night sky background or other noise sources such as lights from airplanes. The TF scans over hits in the camera (as identified by the SDFs) in subarrays of 5 × 5 PMTs. The subarray window scans over all cameras at a given observatory site for 25.6 μs search window every 12.8 μs. Those patterns observed are compared with the lookup table for possible track recognition. At the same time, the TF module receives "non-conditional" (NC) trigger information from the SDFs, which are set when significantly large signals are found in the PMTs. The TF module can also generate

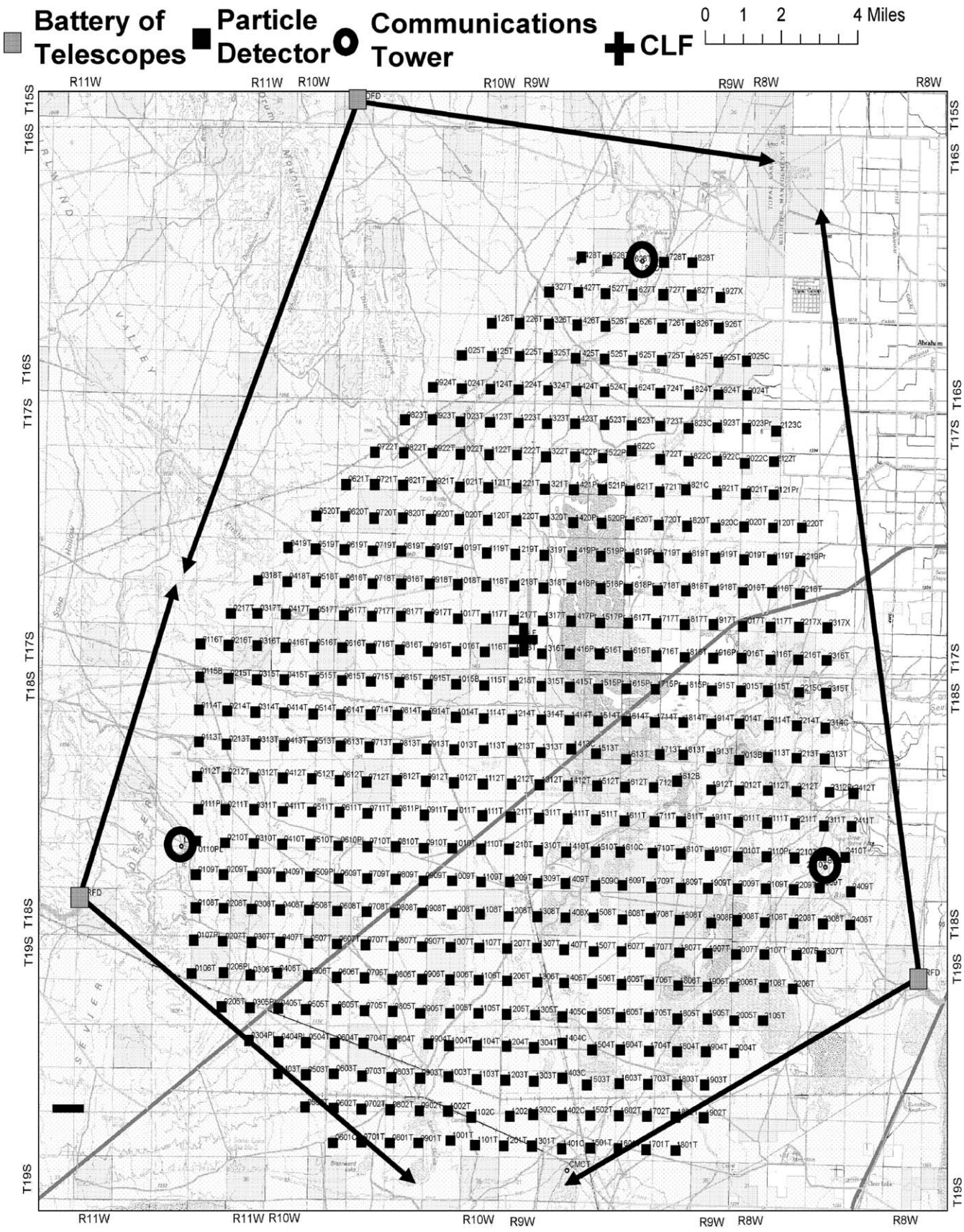

Fig. 1. A map showing the relative locations of the FD stations and the SD array.

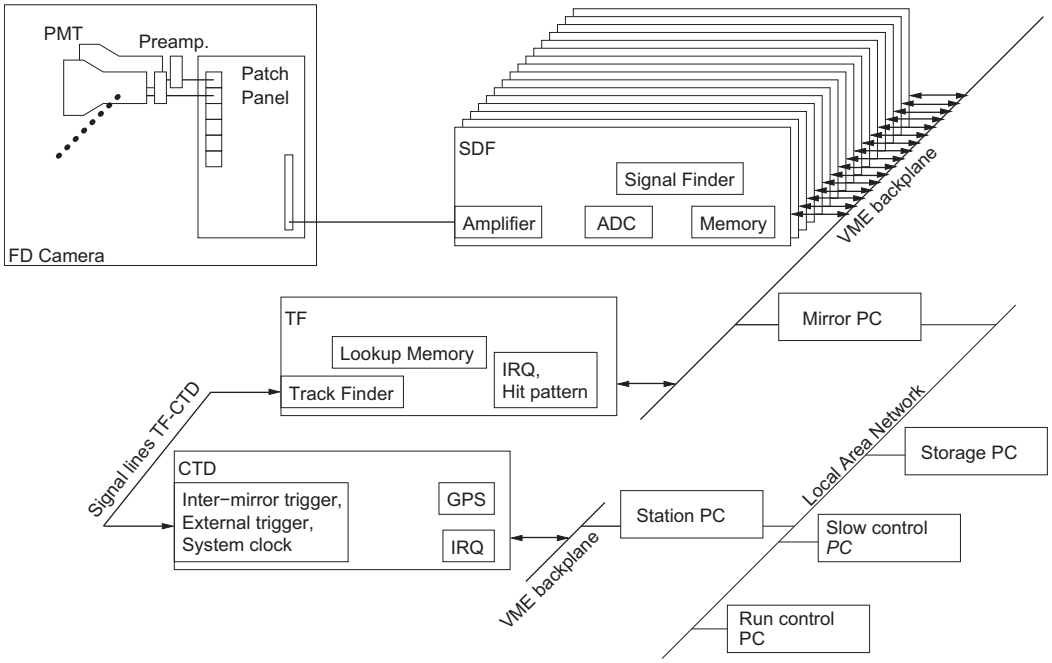

Fig. 2. Block diagram of the electronics and DAQ system of one FD station.

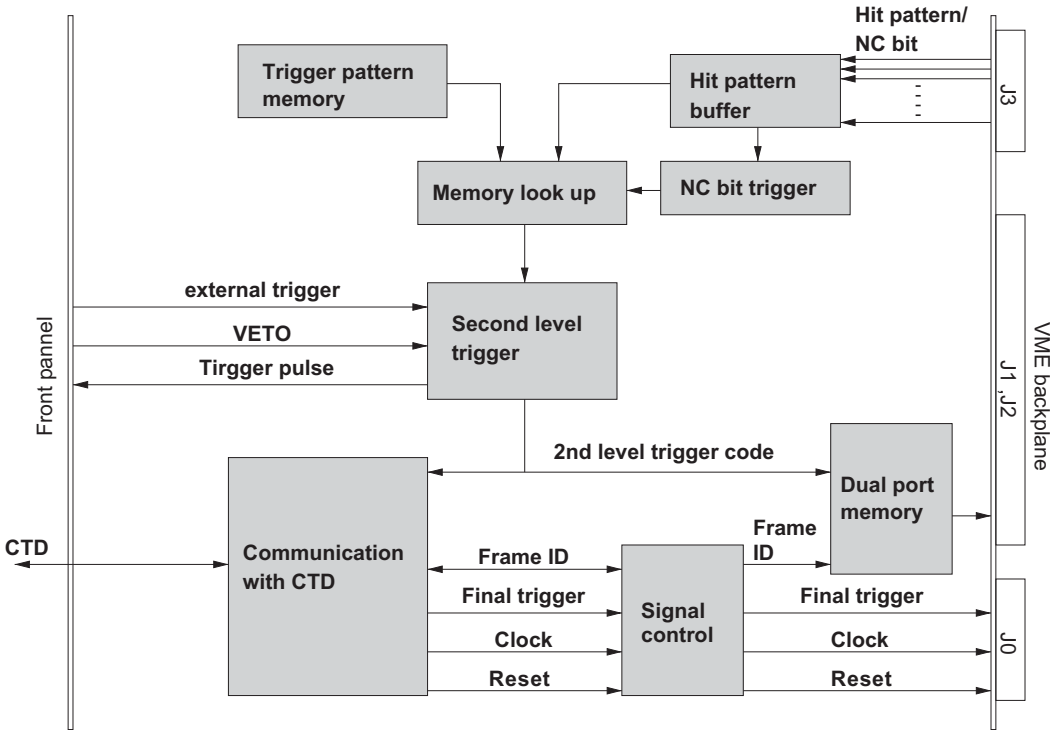

Fig. 3. Block diagram of Telescope Array Track Finder Module.

trigger signals by using the NC information without track identifications for calibration runs. The trigger signals generated by the TF ("second level" triggers) are sent to the CTD module. Each TF has two auxiliary inputs on its front-panel for veto and external triggers, and also has an output pulse indicating a second level trigger.

The track recognition criterion for a "complete track" condition is that five adjoining PMTs in a camera are above threshold within a coincidence window of 25.6 μs, as shown in Fig. 4. The TF crops a hit pattern into a 5×5 sub-matrix and searches for complete tracks in the sub-matrix. The sub-matrix is shifted column by column, row by row across the face of the camera repeating the search for a track. The number of hit patterns of 5×5 pixels is 2^{25}, the lookup table is programmed in the eight static RAMs (CY7C1041, $256\,\mathrm{K} \times 16$). The processing time is $25\,\mathrm{ns} \times 144$ for the pattern matchings of 144 sub-matrices in a camera.

An additional trigger condition implemented in the TF helps it to recognize showers which straddle two cameras leaving short

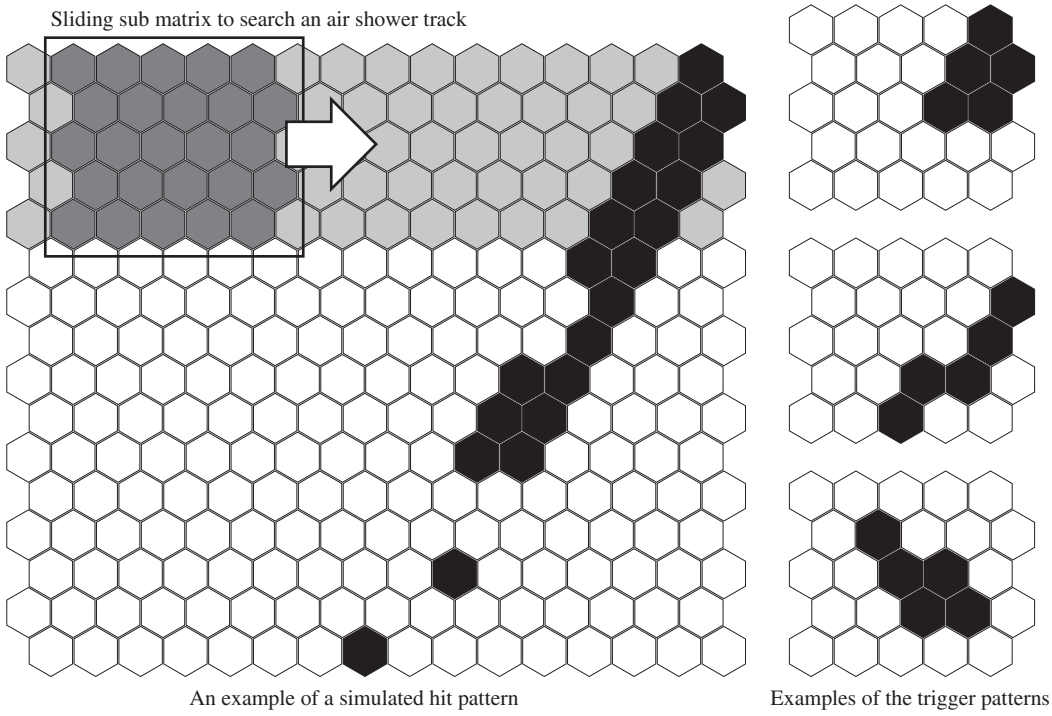

Fig. 4. Schematic diagram of the track finding process.

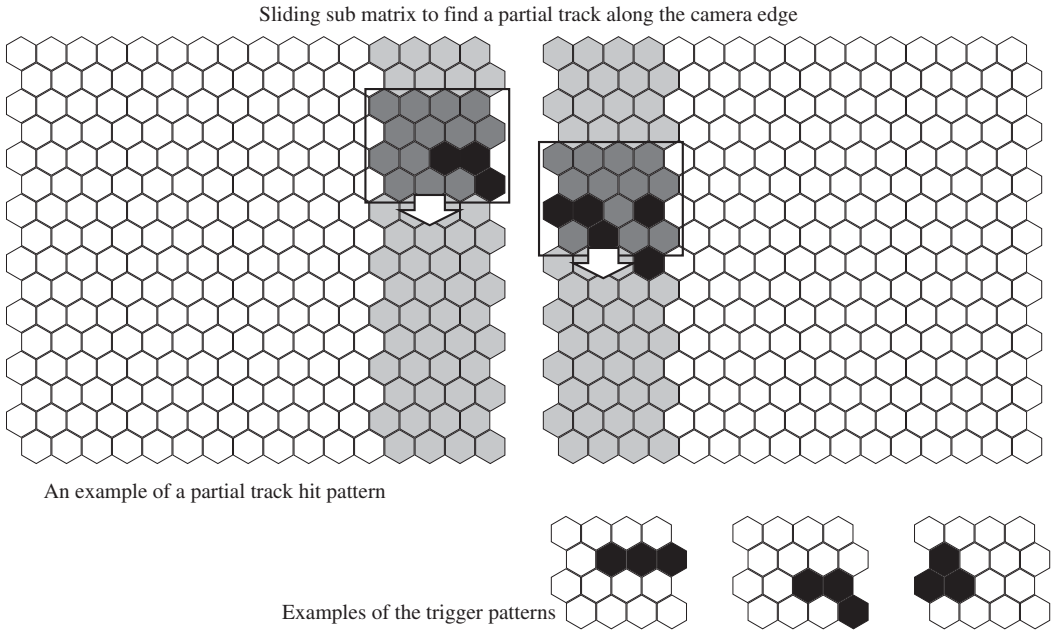

Fig. 5. Schematic diagram of the partial track search near the boundary of a camera.

tracks in each. These "partial tracks" are identified if there are three adjoining PMTs above threshold in a 4×4 sub-matrix at the boundaries of two adjacent cameras (Fig. 5). This is equivalent to the complete track condition, because there is an overlap with a width of one PMT (FOV$\simeq 1^{\circ}$) between the fields of view of two neighboring cameras.

The TF can generate second level triggers in other two cases: first when the NC trigger initiated by a large signal in the SDF and second when an external trigger is induced by a pulse input to the TF front-panel. When one of the trigger criteria is fulfilled, the TF sends the second level trigger information to CTD with a frame ID.

4. The central trigger distributor

The CTD module generates the final trigger for the FD DAQ system to record air shower events. It also serves as the controller of the FD station system distributing the system clock to keep all of the SDFs and the TFs synchronized. It also sends the "reset" signals to initialize the frame counters.

The CTD module is a VME-9U single width board. Its major components are nine CPLD (one XC95288XL and eight XC95144), one FPGA (XC2S200E) and a configuration ROM (XC18V02). A GPS module (Motorola M12 + Timing Oncore (P283T12T1X)) is also

installed on the CTD to provide precise timing of the shower events. The block diagram of CTD is shown in Fig. 6.

The CTD module receives and examines the second level trigger codes from all TFs at an observatory station. When the CTD receives second level triggers with the code of a complete track from one or more TFs, it generates and distributes a "final trigger" to all TFs to record the waveform data of all the PMTs in the station. Aside from this condition, the CTD also triggers the DAQ system when two neighboring TFs send second level triggers with the code of a partial track. The CTD can generate final triggers if TFs send trigger codes of the NC triggers or external triggers for calibration runs, for example to acquire a reference light source to monitor the PMT gain [22]. A final trigger signal consists of a trigger pulse, with a readout mask which is a 12-digit binary number indicating a second level trigger in the telescopes as well as a trigger ID. At the moment of the generation of final trigger signals, the CTD and TFs send IRQ for each VME control PC to start a DAQ cycle.

Event times are calculated from the difference between the rise time of the latest 1 Pulse Per Second (PPS) signal from the GPS module and the beginning of the frame. The time difference is counted with 40 MHz system clock, the resolution of the absolute times is 25 ns. The accuracy of absolute times depends on the stability of 1 PPS signals, which is 20 ns from our measurement.

The time table of a single DAQ cycle, from the beginning of the signal finding process to the end of data transmissions into readout buffers, is shown in Fig. 7. It is dominated by the time required for the track finding process and data transmissions of trigger information between modules. The total process time is smaller than the frame interval of 12.8 μs. If the readout buffers of SDFs and TFs are full, CTD suspends trigger distributions. In order to measure the dead times in operations, the CTD records the IDs and the absolute times of the first and last frame in each suspended period, and also it calculates the sum (length) of these periods. This information is transferred to the VME control PC for the CTD.

5. Aperture of the detectors

In order to evaluate the aperture of our detectors including the electronics and the triggering system described in this paper we performed a series of simulation studies. We developed an FD simulator using real detector parameters (mirror reflectance, quantum efficiencies of PMTs, etc.) and the signal finding procedures in the FD electronics. We carried out air shower simulations to calculate shower development at given atmospheric depths using the Gaisser Hillas formula. We then

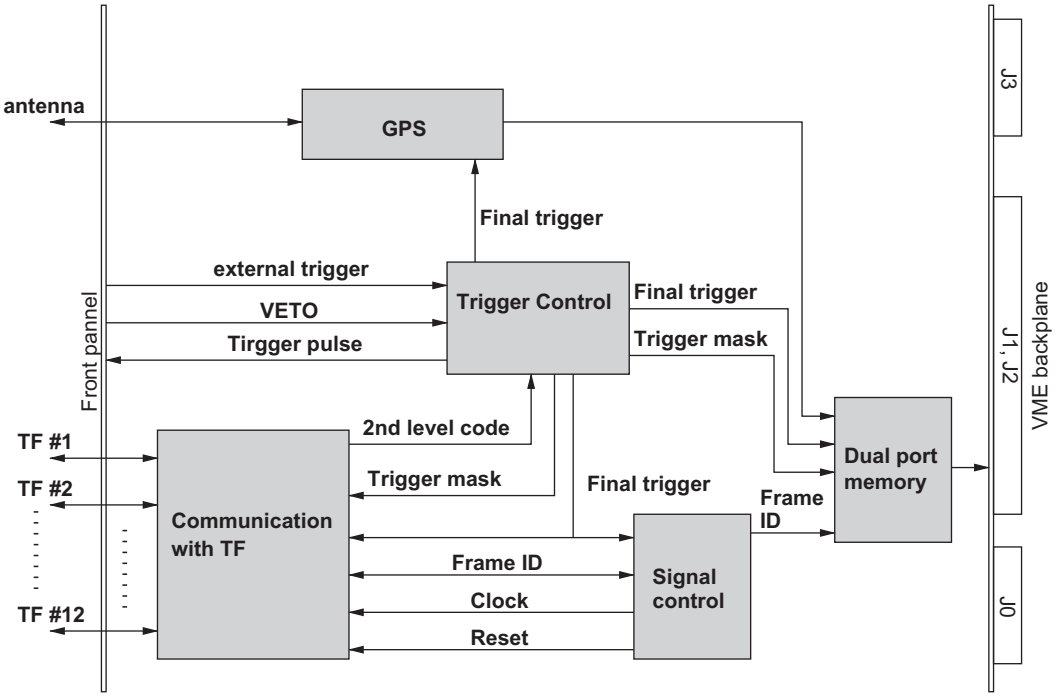

Fig. 6. Block diagram of Telescope Array Central Trigger Distributor module.

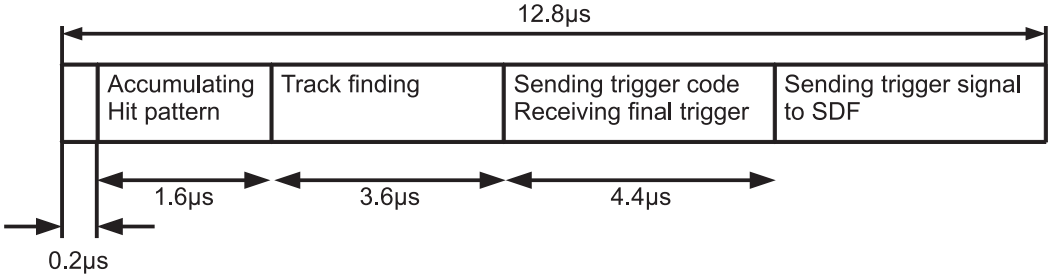

Fig. 7. The time table of a single triggering cycle.

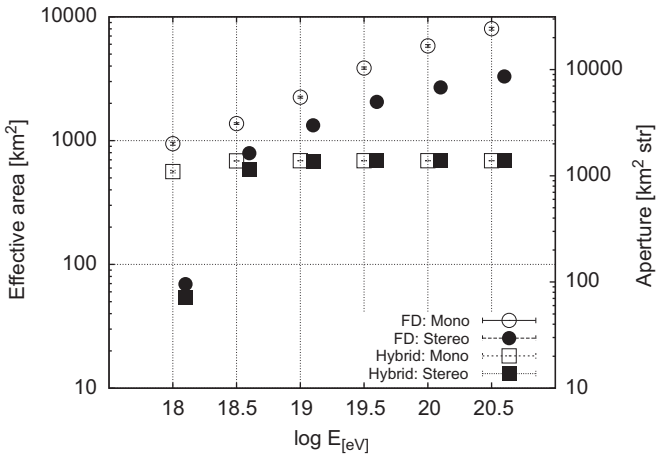

Fig. 8. TA-FD apertures. Open circle: monocular observation (three FD stations), filled circle: stereo observation ($_3C_2$ = three combinations), open square: hybrid-mono observation, filled square: hybrid-stereo observation. (The data points of stereo apertures are slightly shifted to right to make them easier to see.)

evaluated the number of fluorescence photons which would be detected by the PMTs using a ray-tracing technique. The positions of shower impact points were randomly distributed around a station, and the arrival directions of air showers were uniformly distributed in the sky up to the zenith angle θ of 60°. The flux of night sky background (NSB) photons measured at our site was also considered in the simulations.

To evaluate the FD aperture, we first define a "trigger function" of a single telescope, which gives shower detection probabilities as a function of shower core position (R, Φ), where R is the distance of the shower core from the telescope and Φ is the angular distance of the core about the line of sight of the telescope. In calculating the trigger functions, we generated air shower events with different primary energies within the FOV of the telescope, and then examined these events with the triggering criteria. Once the trigger function of a single telescope is obtained, we can evaluate an aperture of a whole FD station by summing up the trigger functions of all the telescopes in the station [23]. Using this method, FD trigger functions can easily be obtained for various detector configurations including monocular observation (air shower detections in one FD station), stereo observation (coincidence detections with two or more FD stations), as well as for hybrid observation (shower detections with the FDs and the SD array).

The FD aperture $A(E)$ as a function of cosmic ray energy E is calculated by using the trigger functions $\varepsilon(R, \Phi; E)$ as

$$A(E) = \int \varepsilon(R, \Phi; E)\cos\theta \, \mathrm{d}\Omega \, \mathrm{d}S \quad (1)$$

where $\mathrm{d}S = R\,\mathrm{d}R\,\mathrm{d}\Phi$, and $\mathrm{d}\Omega$ is an arrival direction of cosmic rays. The FD apertures are shown in Fig. 8 for monocular observation with three FD stations as well as for stereo observation. The hybrid apertures are also shown in the figure, evaluated by replacing the FD trigger function ε by $\varepsilon_{FD} \times \varepsilon_{SD}$. In the calculations, for simplicity, we define the SD trigger efficiency ε_{SD} as 1 (0) for showers with cores inside (outside) an array composed of 576 scintillator surface detectors.[1] It can be seen that the TA hybrid aperture is a constant for cosmic rays with primary energies greater than 10^{19} eV because of the assumption that ε_{SD} is energy-independent.

[1] The original plan called for 576 detectors; however the final number of surface detectors in the array "as built" is 507 (as of 2008).

Note that the apertures calculated here are for "ideal" cases. The actual aperture must take into account conditions during observation including such as atmospheric transparency and its variations, actual PMT gains, NSB photon flux.

6. Conclusion

We have developed trigger electronics for the Telescope Array Experiment. They are designed for the observation of UHECRs with the detections of fluorescence photons with imaging cameras of a large number of PMTs. We began the observation of UHECR air showers in March 2008, and the average trigger rate is about ~3 Hz.

The electronics include a TF module which searches for shower track images on the cameras and the CTD generates event triggers and synchronizes the data acquisition system of the FD station. All the trigger logics are implemented on FPGA, CPLD and RAM devices, which allow trigger modes to be easily exchanged by replacing the driver software for example during calibration runs.

We also developed an efficient method for the evaluations of the FD apertures with a Monte Carlo technique. It is worthy to estimate shower event rates in TA observation. They can be evaluated by assuming cosmic ray energy spectrum and observation efficiency. Here we used the AGASA and the HiRes spectra, and assumed observation time 50 h in a month (observation efficiency 7%). In a case of monocular observation with three FD stations, the expected numbers of events of cosmic rays with energies greater than 10^{20} eV in one-year operation are evaluated as ~10 and ~1 for the AGASA and the HiRes spectrum, respectively. Therefore, with a good energy resolution (~10%) of the TA detectors, we will obtain a conclusive result for the GZK cutoff problem on cosmic ray physics in the first few year observation. Recently the Auger group reported the anisotropy and the energy spectrum of UHECRs [24,25]. TA observation in the northern hemisphere also gives an important clue to clarify the origin of cosmic rays.

Acknowledgments

The Telescope Array Collaboration wishes to acknowledge the support of the Japanese government through a Grant-in-Aid for Scientific Research (Kakenhi) on the Priority Area "The Origin of the Highest Energy Cosmic Rays" as well as the U.S. National Science Foundation (NSF) through Awards PHY-0307098 and PHY-0601915 (University of Utah) and PHY-0305516 (Rutgers University). This work was supported by a 21st Century COE Program at Tokyo Institute of Technology "Nanometer-Scale Quantum Physics" by the Ministry of Education, Culture, Sports, Science and Technology. The Dr. Ezekiel R. and Edna Wattis Dumke Foundation, The Willard L. Eccles Foundation and The George S. and Dolores Dore Eccles Foundation all helped with generous donations. The State of Utah supported the project through its Economic Development Board, and the University of Utah supported us through the Office of the Vice President for Research. We gratefully acknowledge the contributions from the technical staffs of our home institutions. The use of the experimental site became possible by the cooperation of the State of Utah School and Institutional Trust Lands Administration (SITLA), the Federal Bureau of Land Management (BLM) and the United States Air Force. We are deeply grateful to G.N.D. Ltd. and Meisei Electronics Co., Ltd. for their kind support. We also wish to thank the people and the officials of Millard County, Utah, for their steadfast and warm supports.

References

[1] A.A. Penzias, R.W. Wilson, Astrophys. J. 142 (1965) 419.
[2] K. Greisen, Phys. Rev. Lett. 16 (1966) 748.
[3] G.T. Zatsepin, V.A. Kuzmin, Sov. Phys. JETP Lett. 4 (1966) 78.
[4] N. Chiba, et al., Nucl. Instr. and Meth. A 311 (1992) 338.
[5] H. Ohoka, et al., Nucl. Instr. and Meth. A 385 (1997) 268.
[6] M. Takeda, et al., Phys. Rev. Lett. 81 (1998) 1163.
[7] M. Takeda, et al., Astropart. Phys. 19 (2003) 447.
[8] J.N. Matthews, et al., Acta Phys. Polon. B 35 (2004) 1863.
[9] D.R. Bergman, et al., in: Proceedings of 29th ICRC, Pune, vol. 7, 2005, p. 307.
[10] R.U. Abbasi, et al., Phys. Rev. Lett. 100 (2008) 101101.
[11] S. Ozawa, et al., in: Proceedings of 29th ICRC, Pune, vol. 8, 2005, p. 177.
[12] H. Kawai, et al., Nucl. Phys. B (Proc. Suppl.) 175–176 (2008) 221.
[13] S. Ogio, et al., in: Proceedings of 29th ICRC, Pune, vol. 8, 2005, p. 173.
[14] J. Abraham, et al., Nucl. Instr. and Meth. A 523 (2005) 50.
[15] H. Takami, K. Sato, Astrophys. J. 681 (2008) 1279.
[16] M. Takeda, et al., Astrophys. J. 522 (1999) 225.
[17] Y. Uchihori, et al., Astropart. Phys. 13 (2000) 151.
[18] R.U. Abbasi, et al., Astropart. Phys. 22 (2004) 139.
[19] R.U. Abbasi, et al., Astrophys. J. 636 (2006) 280.
[20] J.N. Matthews, et al., in: Proceedings of 30th ICRC, Merida, 2007, p. 1254.
[21] A. Taketa, et al., in: Proceedings of 29th ICRC, Pune, vol. 8, 2005, p. 209.
[22] H. Tokuno, et al., Nucl. Instr. and Meth. A 601 (2009) 364.
[23] Y. Tsunesada, et al., in: Proceedings of 30th ICRC, Merida, 2007, p. 0820.
[24] J. Abraham, et al., Phys. Rev. Lett. 101 (2008) 061101.
[25] The Pierr Auger Collaboration, Science 318 (2007) 5852.